

# The flavor-changing top-charm associated productions at ILC in littlest Higgs model with T parity

Yanju Zhang, Gongru Lu, and Xuelei Wang  
*College of Physics and Information Engineering,*  
*Henan Normal University, Xinxiang, Henan 453007, P.R. China*  
(Dated: December 5, 2018)

The littlest Higgs model with T-parity (LHT) has new flavor-changing (FC) couplings with the Standard Model (SM) quarks, which do not suffer strong constraints from electroweak precision data. So these FC interactions may enhance the cross sections of some flavor-changing neutral-current (FCNC) processes. In this work, we study the FC top-charm associated productions via  $e^- \gamma$  collision at the ILC. We find that the cross sections are sensitive to the mirror quark masses. With reasonable values of the parameters, the cross sections may reach the detectable level and provide useful information about the relevant parameters in the LHT model, especially setting an upper limit on the mirror quark masses.

PACS numbers: 14.65.Ha, 12.60.-i, 12.15.Mm, 13.85.Lg

## I. INTRODUCTION

An interesting solution to the hierarchy problem of the Standard Model (SM) is the little Higgs theory [1]. In this theory the Higgs boson is regarded as a pseudo-Goldstone boson (PGB) which can be naturally "little" in the current reincarnation of the PGB idea called collective symmetry breaking. Through such a collective symmetry breaking mechanism, the one loop quadratic divergences in the Higgs boson mass can be avoided. The littlest Higgs model (LH) [2] is the most economical implementation of the little Higgs idea, which, however, suffers strong constraints from electroweak precision data [3] due to the tree level mixing of heavy and light mass eigenstates. So the LH model would require raising the mass scale and thus reintroduce the fine-tuning in the Higgs potential [4]. To solve this problem, a  $Z_2$  discrete symmetry called T-parity is introduced [5]. Under this T-parity the SM particles are even while most of the new particles at the TeV scale are odd. T-parity explicitly forbids any tree-level contribution from the heavy gauge bosons to the observables involving only SM particles as external states. Since in the LHT model the corrections to the precision electroweak observables are generated at loop-level and suppressed, the fine tuning can be avoided [6].

It is well known that the flavor-changing neutral-current (FCNC) interactions are absent at tree level and extremely small at loop levels in the SM due to the GIM mechanism. However, in the LHT model, the flavor-changing (FC) interactions between the SM fermions and the mirror fermions, which are parameterized by the newly CKM-like unitary mixing matrices, may have significant contributions to some FC processes. So much attention was paid on the FC interactions in LHT model in recent years. Firstly, the LHT flavor structure was analysed and some constraints on the mirror fermion mass spectrum was obtained from an one-loop analysis of neutral meson mixing in the  $K, B$  and  $D$  systems [7]. Then an extensive study of FC transitions in the LHT model was performed in [8–10], which considered all prominent rare  $K$  and  $B$  decays and presented a collection of Feynman rules to the order of  $v^2/f^2$ . Motivated by the experimental evidence of meson oscillations in the  $D$ -system, the impact of  $D^0 - \bar{D}^0$  mixing on the LHT flavor structure was investigated in [11]. Furthermore, the LHT flavor study was extended to the lepton flavor violating decays in [12].

The International Linear Collider (ILC) with the center of mass (c.m.) energy from 200 GeV to 1.0 TeV and high luminosity has been proposed [13]. Due to its rather clean environment and high luminosity, the ILC will be an ideal machine for probing new physics. In such a collider, in addition to  $e^+e^-$  collision, we may also realize  $\gamma\gamma$  or  $e^- \gamma$  collision with the photon beams generated by the backward Compton scattering of incident electron- and laser-beams [14]. In particular, as the heaviest fermion with a mass of the order of the electroweak scale, the top quark is naturally regarded to be more sensitive to new physics than other fermions. Therefore the top quark FCNC processes at the ILC would provide an important test for new physics. This stimulates many attempts in probing new physics via rare top quark decays [15] or FC production processes at ILC [16–26]. The FC couplings between the SM fermions and the mirror fermions can also induce the loop-level  $tcV$  ( $V = \gamma, Z, g$ ) couplings in the LHT model. Studies [27–29] showed that some processes induced by such  $tcV$  couplings in the LHT model can be significantly

enhanced. In this paper, we will study the process  $e^- \gamma \rightarrow e^- t \bar{c}$  induced by the  $tcV$  couplings in the LHT model and compare with the process  $e^+ e^- (\gamma \gamma) \rightarrow t \bar{c}$  studied previously[28]. Note that these processes have been studied thoroughly in other models, such as the MSSM [16, 17], the 2HDM[18, 19] and the TC2 model[20–22], and also in the model-independent way [23–25]. They showed that the production rates of such processes could be significantly enhanced by several orders compared to the SM predictions [16, 30]. As found in other new physics models [16, 20], the process  $e^- \gamma \rightarrow e^- t \bar{c}$  has a much larger rate than  $e^+ e^- \rightarrow t \bar{c}$  for some part of the parameter space. In our study we will compare the LHT prediction with those predicted by other new physics models. Such an analysis will help to distinguish different models once the measurements are observed at the ILC.

This paper is organized as follows. In Sec.II, we briefly review the LHT model. In Sec.III, we present the detailed calculations for the production processes. The numerical results of the production cross sections and discussions are shown in Sec.IV. Our conclusions are listed in the last section.

## II. THE LITTLEST HIGGS MODEL WITH T-PARITY

The LHT model[5] is based on a non-linear  $\sigma$  model describing an  $SU(5)/SO(5)$  symmetry breaking with a locally gauged sub-group  $[SU(2) \times U(1)]^2$ . The  $SU(5)$  symmetry spontaneously breaks down to  $SO(5)$  at the scale  $f \sim \mathcal{O}(TeV)$ . From the  $SU(5)/SO(5)$  breaking, there arise 14 Nambu-Goldstone bosons which are described by the matrix  $\Pi$ , given explicitly by

$$\Pi = \begin{pmatrix} -\frac{\omega^0}{2} - \frac{\eta}{\sqrt{20}} & -\frac{\omega^+}{\sqrt{2}} & -i\frac{\pi^+}{\sqrt{2}} & -i\phi^{++} & -i\frac{\phi^+}{\sqrt{2}} \\ -\frac{\omega^-}{\sqrt{2}} & \frac{\omega^0}{2} - \frac{\eta}{\sqrt{20}} & \frac{v+h+i\pi^0}{2} & -i\frac{\phi^+}{\sqrt{2}} & \frac{-i\phi^0 + \phi^P}{\sqrt{2}} \\ i\frac{\pi^-}{\sqrt{2}} & \frac{v+h-i\pi^0}{2} & \sqrt{4/5}\eta & -i\frac{\pi^+}{\sqrt{2}} & \frac{v+h+i\pi^0}{2} \\ i\phi^{--} & i\frac{\phi^-}{\sqrt{2}} & i\frac{\pi^-}{\sqrt{2}} & -\frac{\omega^0}{2} - \frac{\eta}{\sqrt{20}} & -\frac{\omega^-}{\sqrt{2}} \\ i\frac{\phi^-}{\sqrt{2}} & \frac{i\phi^0 + \phi^P}{\sqrt{2}} & \frac{v+h-i\pi^0}{2} & -\frac{\omega^+}{\sqrt{2}} & \frac{\omega^0}{2} - \frac{\eta}{\sqrt{20}} \end{pmatrix} \quad (1)$$

Here,  $H = (-i\pi^+ \sqrt{2}, (v+h+i\pi^0)/2)^T$  is the SM Higgs doublet and  $\Phi$  is a physical scalar triplet with

$$\Phi = \begin{pmatrix} -i\phi^{++} & -i\frac{\phi^+}{\sqrt{2}} \\ -i\frac{\phi^+}{\sqrt{2}} & \frac{-i\phi^0 + \phi^P}{\sqrt{2}} \end{pmatrix} \quad (2)$$

In the LHT model, a T-parity discrete symmetry is introduced to make the model consistent with the electroweak precision data. Under the T-parity, the fields  $\Phi, \omega$  and  $\eta$  are odd, and the SM Higgs doublet  $H$  is even.

For the gauge subgroup  $[SU(2) \times U(1)]^2$  of the global symmetry  $SU(5)$ , from the first step of symmetry breaking  $[SU(2) \times U(1)]^2 \rightarrow SU(2)_L \times U(1)_Y$ , which is identified as the SM electroweak gauge group, the Goldstone bosons  $\omega^0, \omega^\pm$  and  $\eta$  are respectively eaten by the new T-odd gauge bosons  $Z_H, W_H$  and  $A_H$ , which obtain masses at the order of  $\mathcal{O}(v^2/f^2)$

$$M_{Z_H} \equiv M_{W_H} = fg(1 - \frac{v^2}{8f^2}), \quad M_{A_H} = \frac{fg'}{\sqrt{5}}(1 - \frac{5v^2}{8f^2}), \quad (3)$$

with  $g, g'$  being the corresponding coupling constants of  $SU(2)_L$  and  $U(1)_Y$ .

From the second step of symmetry breaking  $SU(2)_L \times U(1)_Y \rightarrow U(1)_{em}$ , the masses of the SM T-even gauge bosons  $Z$  and  $W$  are generated through eating the Goldstone bosons  $\pi^0$  and  $\pi^\pm$ . They are given at  $\mathcal{O}(v^2/f^2)$  by

$$M_{W_L} = \frac{gv}{2}(1 - \frac{v^2}{12f^2}), \quad M_{Z_L} = \frac{gv}{2\cos\theta_W}(1 - \frac{v^2}{12f^2}), \quad M_{A_L} = 0. \quad (4)$$

A consistent and phenomenologically viable implementation of T-parity in the fermion sector requires the introduction of mirror fermions. The T-even fermion sector consists of the SM quarks, leptons and an additional heavy quark  $T_+$ . The T-odd fermion sector consists of three generations of mirror quarks

and leptons and an additional heavy quark  $T_-$ . Only the mirror quarks  $(u_H^i, d_H^i)$  are involved in this paper. The mirror fermions get masses

$$\begin{aligned} m_{H_i}^u &= \sqrt{2}\kappa_i f \left(1 - \frac{v^2}{8f^2}\right) \equiv m_{H_i} \left(1 - \frac{v^2}{8f^2}\right), \\ m_{H_i}^d &= \sqrt{2}\kappa_i f \equiv m_{H_i}, \end{aligned} \quad (5)$$

where the Yukawa couplings  $\kappa_i$  can in general depend on the fermion species  $i$ .

The mirror fermions induce a new flavor structure and there are four CKM-like unitary mixing matrices in the mirror fermion sector:

$$V_{H_u}, \quad V_{H_d}, \quad V_{H_l}, \quad V_{H_\nu}. \quad (6)$$

These mirror mixing matrices are involved in the FC interactions between the SM fermions and the T-odd mirror fermions which are mediated by the T-odd heavy gauge bosons or the Goldstone bosons.  $V_{H_u}$  and  $V_{H_d}$  satisfy the relation

$$V_{H_u}^\dagger V_{H_d} = V_{CKM}. \quad (7)$$

We parameterize the  $V_{H_d}$  with three angles  $\theta_{12}^d, \theta_{23}^d, \theta_{13}^d$  and three phases  $\delta_{12}^d, \delta_{23}^d, \delta_{13}^d$

$$V_{H_d} = \begin{pmatrix} c_{12}^d c_{13}^d & s_{12}^d c_{13}^d e^{-i\delta_{12}^d} & s_{13}^d e^{-i\delta_{13}^d} \\ -s_{12}^d c_{23}^d e^{i\delta_{12}^d} - c_{12}^d s_{23}^d s_{13}^d e^{i(\delta_{13}^d - \delta_{23}^d)} & c_{12}^d c_{23}^d - s_{12}^d s_{23}^d s_{13}^d e^{i(\delta_{13}^d - \delta_{12}^d - \delta_{23}^d)} & s_{23}^d c_{13}^d e^{-i\delta_{23}^d} \\ s_{12}^d s_{23}^d e^{i(\delta_{12}^d + \delta_{23}^d)} - c_{12}^d c_{23}^d s_{13}^d e^{i\delta_{13}^d} & -c_{12}^d s_{23}^d e^{i\delta_{23}^d} - s_{12}^d c_{23}^d s_{13}^d e^{i(\delta_{13}^d - \delta_{12}^d)} & c_{23}^d c_{13}^d \end{pmatrix} \quad (8)$$

The matrix  $V_{H_u}$  is then determined through  $V_{H_u} = V_{H_d} V_{CKM}^\dagger$ . As in the case of the CKM matrix the angles  $\theta_{ij}^d$  can all be made to lie in the first quadrant with  $0 \leq \delta_{12}^d, \delta_{23}^d, \delta_{13}^d < 2\pi$ .

### III. TOP-CHARM QUARK ASSOCIATED PRODUCTIONS IN THE LHT MODEL

In the LHT model, there are FC interactions between SM quarks and T-odd mirror quarks which are mediated by the heavy T-odd gauge bosons or Goldstone bosons. With these FC couplings, the loop-level FC couplings  $t\bar{c}\gamma(Z)$  can be induced and the relevant Feynman diagrams are shown in Fig.1.

The effective one-loop level couplings  $t\bar{c}\gamma(Z)$  can be directly calculated by the method introduced in Ref.[31]. The relevant Feynman rules can be found in Ref.[9]. We list the explicit forms of  $\Gamma_{t\bar{c}\gamma}^\mu(p_t, p_{\bar{c}})$  and  $\Gamma_{t\bar{c}Z}^\mu(p_t, p_{\bar{c}})$  in Appendix.

The FC couplings  $t\bar{c}\gamma(Z)$  can contribute to the top-charm associated productions. Here we reconsider the processes  $e^+e^- \rightarrow t\bar{c}$  in  $e^+e^-$  collision and  $\gamma\gamma \rightarrow t\bar{c}$  in  $\gamma\gamma$  collision which have been calculated in the literature[28], since we had a mistake in the program calculation of them before. So we will no longer present the relevant Feynman diagrams and the corresponding production amplitudes of the processes in the following.

We also focus on the process  $e^-\gamma \rightarrow e^-\bar{c}$  in  $e^-\gamma$  collision. The  $t\bar{c}$  production in  $e^-\gamma$  collision proceeds through the process  $e^-\gamma \rightarrow e^-\gamma^*(Z^*)\gamma \rightarrow e^-\bar{c}$ , where the  $\gamma$ -beam is generated by the backward Compton scattering of incident electron- and laser-beam and the  $\gamma^*(Z^*)$  is radiated from  $e^-$  beam. The corresponding Feynman diagram is shown in Fig.2(A-E) and the invariant production amplitudes of the process can be written as

$$\begin{aligned} M_A^\gamma &= -e^2 G(p_1 + p_2, 0) G(p_3 + p_4, 0) \bar{u}_{e^-}(p_5) \gamma_\mu (\not{p}_1 + \not{p}_2) \not{\epsilon}(p_2) u_{e^-}(p_1) \\ &\quad \times \bar{u}_t(p_3) \Gamma_{t\bar{c}\gamma}^\mu(p_3, p_4) v_{\bar{c}}(p_4), \end{aligned} \quad (9)$$

$$\begin{aligned} M_A^Z &= \frac{eg}{\cos\theta_W} G(p_1 + p_2) G(p_3 + p_4, M_Z) \bar{u}_{e^-}(p_5) \gamma_\mu \left[ -\frac{1}{2} + \sin^2\theta_W \right] P_L \\ &\quad + (\sin^2\theta_W) P_R (\not{p}_1 + \not{p}_2) \not{\epsilon}(p_2) u_{e^-}(p_1) \bar{u}_t(p_3) \Gamma_{t\bar{c}Z}^\mu(p_3, p_4) v_{\bar{c}}(p_4), \end{aligned} \quad (10)$$

$$M_B^\gamma = \frac{2e^2}{3}G(p_1 - p_5, 0)G(p_2 - p_4, m_c)\bar{u}_{e^-}(p_5)\gamma_\mu u_{e^-}(p_1) \\ \times \bar{u}_t(p_3)\Gamma_{t\bar{c}\gamma}^\mu(p_3, p_4 - p_2)(\not{p}_2 - \not{p}_4 + m_c)\not{\epsilon}(p_2)v_{\bar{c}}(p_4), \quad (11)$$

$$M_B^Z = -\frac{2eg}{3\cos\theta_W}G(p_1 - p_5, M_Z)G(p_2 - p_4, m_c)\bar{u}_{e^-}(p_5)\gamma_\mu\left[-\frac{1}{2} + \sin^2\theta_W\right]P_L \\ + (\sin^2\theta_W)P_R]u_{e^-}(p_1)\bar{u}_t(p_3)\Gamma_{t\bar{c}Z}^\mu(p_3, p_4 - p_2)(\not{p}_2 - \not{p}_4 + m_c)\not{\epsilon}(p_2)v_{\bar{c}}(p_4), \quad (12)$$

$$M_C^\gamma = \frac{2e^2}{3}G(p_1 - p_5, 0)G(p_2 - p_4, m_t)\bar{u}_{e^-}(p_5)\gamma_\mu u_{e^-}(p_1) \\ \times \bar{u}_t(p_3)\gamma^\mu(\not{p}_2 - \not{p}_4 + m_t)\Gamma_{t\bar{c}\gamma}^\nu(p_2 - p_4, p_4)\epsilon_\nu(p_2)v_{\bar{c}}(p_4), \quad (13)$$

$$M_C^Z = -\frac{g^2}{\cos^2\theta_W}G(p_1 - p_5, M_Z)G(p_2 - p_4, m_t)\bar{u}_{e^-}(p_5)\gamma_\mu\left[-\frac{1}{2} + \sin^2\theta_W\right]P_L \\ + (\sin^2\theta_W)P_R]u_{e^-}(p_1)\bar{u}_t(p_3)\gamma^\mu\left[\left(\frac{1}{2} - \frac{2}{3}\sin^2\theta_W\right)P_L - \frac{2}{3}(\sin^2\theta_W)P_R\right] \\ \times (\not{p}_2 - \not{p}_4 + m_t)\Gamma_{t\bar{c}\gamma}^\nu(p_2 - p_4, p_4)\epsilon_\nu(p_2)v_{\bar{c}}(p_4), \quad (14)$$

$$M_D^\gamma = \frac{2e^2}{3}G(p_1 - p_5, 0)G(p_3 - p_2, m_t)\bar{u}_{e^-}(p_5)\gamma_\mu u_{e^-}(p_1) \\ \times \bar{u}_t(p_3)\not{\epsilon}(p_2)(\not{p}_3 - \not{p}_2 + m_t)\Gamma_{t\bar{c}\gamma}^\mu(p_3 - p_2, p_4)v_{\bar{c}}(p_4), \quad (15)$$

$$M_D^Z = -\frac{2eg}{3\cos\theta_W}G(p_1 - p_5, M_Z)G(p_3 - p_2, m_t)\bar{u}_{e^-}(p_5)\gamma_\mu\left[-\frac{1}{2} + \sin^2\theta_W\right]P_L \\ + (\sin^2\theta_W)P_R]u_{e^-}(p_1)\bar{u}_t(p_3)\not{\epsilon}(p_2)(\not{p}_3 - \not{p}_2 + m_t)\Gamma_{t\bar{c}Z}^\mu(p_3 - p_2, p_4)v_{\bar{c}}(p_4), \quad (16)$$

$$M_E^\gamma = \frac{2e^2}{3}G(p_1 - p_5, 0)G(p_3 - p_2, m_c)\bar{u}_{e^-}(p_5)\gamma_\mu u_{e^-}(p_1) \\ \times \bar{u}_t(p_3)\Gamma_{t\bar{c}\gamma}^\nu(p_3, p_2 - p_3)\epsilon_\nu(p_2)(\not{p}_3 - \not{p}_2 + m_c)\gamma^\mu v_{\bar{c}}(p_4), \quad (17)$$

$$M_E^Z = -\frac{g^2}{\cos^2\theta_W}G(p_1 - p_5, M_Z)G(p_3 - p_2, m_c)\bar{u}_{e^-}(p_5)\gamma_\mu\left[-\frac{1}{2} + \sin^2\theta_W\right]P_L \\ + (\sin^2\theta_W)P_R]u_{e^-}(p_1)\bar{u}_t(p_3)\Gamma_{t\bar{c}\gamma}^\nu(p_3, p_2 - p_3)\epsilon_\nu(p_2)(\not{p}_3 - \not{p}_2 + m_c)\gamma^\mu \\ \times \left[\left(\frac{1}{2} - \frac{2}{3}\sin^2\theta_W\right)P_L - \frac{2}{3}(\sin^2\theta_W)P_R\right]v_{\bar{c}}(p_4), \quad (18)$$

where  $P_L = \frac{1}{2}(1 - \gamma_5)$  and  $P_R = \frac{1}{2}(1 + \gamma_5)$  are the left and right chirality projectors.  $p_1, p_2$  are the momenta of the incoming  $e^-, \gamma$ , and  $p_3, p_4, p_5$  are the momenta of the outgoing final states top quark, anti-charm quark and electron, respectively. We also define  $G(p, m)$  as  $\frac{1}{p^2 - m^2}$ .

With the above amplitudes, we can directly obtain the production cross section  $\hat{\sigma}(\hat{s})$  for the subprocess  $e^-\gamma \rightarrow e^-\bar{t}\bar{c}$  and the total cross sections at the  $e^+e^-$  linear collider can be obtained by folding  $\hat{\sigma}(\hat{s})$  with the photon distribution function  $F(x)$  [32]:

$$\sigma_{e^-\gamma \rightarrow e^-\bar{t}\bar{c}}(s_{e^+e^-}) = \int_{(m_t+m_c)^2/s_{e^+e^-}}^{x_{max}} dx F(x) \hat{\sigma}(\hat{s}) \quad (19)$$

where  $s$  is the c.m. energy squared for  $e^+e^-$ . The subprocess occurs effectively at  $\hat{s} = xs$ , and  $x$  is the fractions of the electron energies carried by the photons. The explicit form of the photon distribution function  $F(x)$  is

$$F(x) = \frac{1}{D(\xi)} \left[ 1 - x + \frac{1}{1-x} - \frac{4x}{\xi(1-x)} + \frac{4x^2}{\xi^2(1-x)^2} \right], \quad (20)$$

with

$$D(\xi) = \left( 1 - \frac{4}{\xi} - \frac{8}{\xi^2} \right) \ln(1 + \xi) + \frac{1}{2} + \frac{8}{\xi} - \frac{1}{2(1 + \xi)^2}, \quad (21)$$

and

$$\xi = \frac{4E_0\omega_0}{m_e^2}. \quad (22)$$

$E_0$  and  $\omega_0$  are the incident electron and laser light energies, and  $x = \omega/E_0$ . The energy  $\omega$  of the scattered photon depends on its angle  $\theta$  with respect to the incident electron beam and is given by

$$\omega = \frac{E_0(\frac{\xi}{1+\xi})}{1 + (\frac{\theta}{\theta_0})^2}. \quad (23)$$

Therefore, at  $\theta = 0$ ,  $\omega = E_0\xi/(1 + \xi) = \omega_{max}$  is the maximum energy of the backscattered photon, and  $x_{max} = \frac{\omega_{max}}{E_0} = \frac{\xi}{1+\xi}$ .

To avoid unwanted  $e^+e^-$  pair production from the collision between the incident and back-scattered photons, we should not choose too large  $\omega_0$ . The threshold for  $e^+e^-$  pair creation is  $\omega_{max}\omega_0 > m_e^2$ , so we require  $\omega_{max}\omega_0 \leq m_e^2$ . Solving  $\omega_{max}\omega_0 = m_e^2$ , we find

$$\xi = 2(1 + \sqrt{2}) = 4.8. \quad (24)$$

For the choice  $\xi = 4.8$ , we obtain  $x_{max} = 0.83$  and  $D(\xi_{max}) = 1.8$ .

In the above we have ignored the possible polarization for the photon and electron beams and we also assume that the number of the backscattered photons produced per electron is one.

#### IV. THE NUMERICAL RESULTS AND DISCUSSIONS

In our numerical calculations, the charge conjugate  $\bar{t}c$  production channel has also been included. To obtain the numerical results, we take the SM parameters as  $m_t = 171.2$  GeV,  $m_c = 1.25$  GeV,  $s_W^2 = 0.231$ ,  $M_Z = 91.2$  GeV,  $\alpha_e = 1/128$ . Moreover, the LHT model has several free parameters which are related to our study. They are the breaking scale  $f$ , 6 parameters ( $\theta_{12}^d$ ,  $\theta_{13}^d$ ,  $\theta_{23}^d$ ,  $\delta_{12}^d$ ,  $\delta_{13}^d$ ,  $\delta_{23}^d$ ) in the mixing matrix  $V_{H_u}$  and  $V_{H_d}$ , and the masses of the mirror quarks. For the mirror quark masses, we get  $m_{H_i}^u = m_{H_i}^d = m_{H_i}$  ( $i = 1, 2, 3$ ) at  $\mathcal{O}(v/f)$  from Eq.(13). For the matrices  $V_{H_u}$  and  $V_{H_d}$ , considering the regions of parameter space that only loosely constraint the mass spectrum of the mirror fermions[7], we choose two scenarios as in Ref.[28].

$$\text{Case I: } V_{H_d} = 1, \quad V_{H_u} = V_{CKM}^\dagger,$$

$$\text{Case II: } s_{23}^d = 1/\sqrt{2}, \quad s_{12}^d = s_{13}^d = 0, \quad \delta_{12}^d = \delta_{23}^d = \delta_{13}^d = 0.$$

In both cases, the constraints on the mass spectrum of the mirror fermions are very relaxed. On the other hand, Ref.[33] has shown that the experimental bounds on four-fermi interactions involving SM fields provide an upper bound on the mirror fermion masses and this yields  $m_{H_i} \leq 4.8f^2$ . We also consider such constraint in our calculation. For the breaking scale  $f$ , we take two typical values: 500 GeV and 1000 GeV.

For the c.m. energies of the ILC, we choose  $\sqrt{s} = 500, 1000$  GeV as examples. Taking account of the detector acceptance, we have taken the basic cuts on the transverse momentum( $p_T$ ) and the pseudo-rapidity( $\eta$ ) for the final state particles

$$p_T \geq 20\text{GeV}, \quad |\eta| \leq 2.5.$$

The numerical results of the cross sections are summarized in Figs.3-5. Figs.3 and 4 show the cross sections of the processes  $e^+e^-(\gamma\gamma) \rightarrow t\bar{c}$  and  $e^-\gamma \rightarrow e^-t\bar{c}$  as a function of  $m_{H_3}$  for Case I and Case II, respectively.

In Case I, due to the absence of the mixing in the down type gauge and Goldstone boson interactions, there are no constraints on the masses of the mirror quarks at one loop-level from the  $K$  and  $B$  systems and the constraints come only from the  $D$  system. The constraints on the mass of the third generation mirror quark are very weak. Considering the constraint  $m_{H_i} \leq 4.8f^2$ , we take  $m_{H_3}$  to vary in the range of 500-1200 GeV for  $f=500$  GeV and 500-4800 GeV for  $f=1000$  GeV, and fix  $m_{H_1} = m_{H_2} = 500$  GeV.

As shown in Fig.3, the cross sections of the three different production processes rise with the increase of  $m_{H_3}$ . The reason is that the couplings between the mirror quarks and the SM quarks are proportional to the masses of the mirror quarks. The masses of the heavy gauge bosons and the mirror quarks,  $M_{V_H}$  and  $m_{H_i}$ , are proportional to  $f$ , but the scale  $f$  is insensitive to the cross sections of these processes because the production amplitudes are represented in the form of  $m_{H_i}/M_{V_H}$  which cancels the effect of  $f$ . For the case of  $\sqrt{s} = 1000$  GeV, our calculations show this case has the slightly larger effects relative to the case of  $\sqrt{s} = 500$  GeV.

For Case II, the dependence of the cross sections on  $m_{H_3}$  is presented in Fig.4. In this case, the constraints from the  $K$  and  $B$  systems are also very weak. Compared to Case I, the mixing between the second and third generations is enhanced with the choice of a bigger mixing angle  $s_{23}^d$ . Here, we take the same values of  $\sqrt{s}$ ,  $f$  and  $m_{H_i}$  as in Case I. Even with stricter constraints on the masses of the mirror quarks, the large masses of the mirror quarks can also enhance the cross sections significantly. The dependence of the cross sections on the c.m. energy is similar to that in Case I.

Among the three processes from Case I and case II, we find that the cross section of process  $\gamma\gamma \rightarrow t\bar{c}$  is the largest with  $\sqrt{s}, f = 1000$  GeV and heavy mirror quarks. The optimum value of  $\sigma(\gamma\gamma \rightarrow t\bar{c})$  can reach  $\mathcal{O}(10^0)$  fb. On the other hand, the maximal value of cross section for process  $e^-\gamma \rightarrow e^-t\bar{c}$  can reach 0.7 fb, which is higher than that in some models such as MSSM model and type III two Higgs doublet models, but lower than that in TC2 model[20].

In Fig.5 we show the behavior of the cross sections for  $\gamma\gamma \rightarrow t\bar{c}$ ,  $e^-\gamma \rightarrow e^-t\bar{c}$  and  $e^+e^- \rightarrow t\bar{c}$  versus the collider energy for two Cases. We see that the cross section of  $e^+e^- \rightarrow t\bar{c}$  drops quickly with the increase of collider energy. This is because that the contributions of the LHT model come from s-channel, so the large c.m. energy  $\sqrt{s}$  depresses the cross section. However, for the process  $\gamma\gamma \rightarrow t\bar{c}$ , there is only t-channel contributions, so the large c.m. energy can enhance the cross section.

In practice, if we assume conservatively that the signal is reduced to 10% to eliminate backgrounds, we may expect that the production  $\gamma\gamma \rightarrow t\bar{c}$  as large as  $5fb$  may be accessible at the ILC at the  $3\sigma$  level. According to the ILC Reference Design Report [13], the total luminosity is required to be around  $500fb^{-1}$  within the first four years and about  $1000fb^{-1}$  during the first phase of operation. It means that the increment of mirror quark masses can sharply enhance the cross sections of  $\gamma\gamma \rightarrow t\bar{c}$  and  $e^-\gamma \rightarrow e^-t\bar{c}$  to the accessible level at the ILC. On the other hand, the precise measurement of the cross sections can certainly provide some information about mirror quark masses.

Now we discuss the potential to distinguish the different new physics models via the top-charm production at the ILC. The maximal values of the cross sections of the processes  $\gamma\gamma \rightarrow t\bar{c}$ ,  $e^-\gamma \rightarrow e^-t\bar{c}$  and  $e^+e^- \rightarrow t\bar{c}$  in various models are shown in Table 1.

Table 1: The maximal values of the cross sections of the processes  $\gamma\gamma \rightarrow t\bar{c}$ ,  $e^-\gamma \rightarrow e^-t\bar{c}$  and  $e^+e^- \rightarrow t\bar{c}$  in various models (in fb)

	SM	2HDM-III	MSSM	TC2	LHT
$\gamma\gamma \rightarrow t\bar{c}$	$\mathcal{O}(10^{-8})$ [16]	$\mathcal{O}(10^{-1})$ [19]	$\mathcal{O}(10^{-1})$ [16]	$\mathcal{O}(10)$ [20]	$\mathcal{O}(10^0)$
$e^-\gamma \rightarrow e^-t\bar{c}$	$\mathcal{O}(10^{-9})$ [16]	$\mathcal{O}(10^{-2})$ [20]	$\mathcal{O}(10^{-2})$ [16]	$\mathcal{O}(1)$ [20]	$\mathcal{O}(10^{-1})$
$e^+e^- \rightarrow t\bar{c}$	$\mathcal{O}(10^{-10})$ [30]	$\mathcal{O}(10^{-3})$ [18]	$\mathcal{O}(10^{-2})$ [16]	$\mathcal{O}(10^{-1})$ [21]	$\mathcal{O}(10^{-2})$

From Table 1 we see that the new physics models can enhance the SM rates of the FCNC top-charm production processes by several orders because the tree-level FCNC is absent in the SM. The relation of the cross section is  $\sigma(\gamma\gamma \rightarrow t\bar{c}) > \sigma(e^-\gamma \rightarrow e^-t\bar{c}) > \sigma(e^+e^- \rightarrow t\bar{c})$  in every new physics model. Due to the different values of the cross sections, so the top-charm production also provides a good way to distinguish the LHT model from other new physics models.

## V. CONCLUSION

We studied the top-charm associated productions via  $e^+e^-$ ,  $e^-\gamma$  and  $\gamma\gamma$  collisions in the framework of the LHT model at the ILC. The numerical results showed that the cross sections of the processes increase sharply as the mirror quark masses increase, and in a large part of the allowed parameter space, the cross sections of  $\gamma\gamma \rightarrow t\bar{c}$  and  $e^-\gamma \rightarrow e^-t\bar{c}$  may reach the detectable level at the ILC. If these processes can be observed, some information about the FC couplings can be obtained in order to distinguish the LHT model from other new physics. If these FC processes are not to be observed, the upper limit on mirror quark masses can then be given.

## VI. ACKNOWLEDGMENTS

Y. J. Zhang thanks Junjie Cao and Jinmin Yang for useful discussions. This work is supported by the National Natural Science Foundation of China under Grant Nos. 10775039 and 10975047.

- 
- [1] N. Arkani-Hamed, A. G. Cohen and H. Georgi, Phys. Lett. B**513**, 232 (2001); N. Arkani-Hamed, et al., JHEP **0208**, 020 (2002).
  - [2] N. Arkani-Hamed, A. G. Cohen, E. Katz, A. E. Nelson, JHEP **0207**, 034 (2002).
  - [3] J. L. Hewett, F. J. Petriello, and T. G. Rizzo, JHEP **0310**, 062(2003); C. Csaki, et al., Phys. Rev. D**67**, 115002 (2003); Phys. Rev. D**68**, 035009 (2003); M. C. Chen, S. Dawson, Phys. Rev. D**70**, 015003 (2004); W. Kilian and J. Reuter, Phys. Rev. D**70**, 015004 (2004).
  - [4] G. Marandella, C. Schappacher, and A. Strumia, Phys. Rev. D**72**, 035014 (2005).
  - [5] I. Low, JHEP **0410**, 067 (2004); H. C. Cheng and I. Low, JHEP, **0408**, 061 (2004); J. Hubisz and P.Meade, Phys. Rev. D**71**, 035016 (2005); J. Hubisz, S. J. Lee and G. Paz, JHEP **0606**, 041 (2006).
  - [6] J. Hubisz, P. Meade, A. Noble, and M. Perelstein, JHEP **0601**, 136 (2006);
  - [7] J. Hubisz, S. J. Lee and G. Paz, JHEP **0606**, 041 (2006).
  - [8] M. Blanke, *et al.*, JHEP **0612**, 003 (2006).
  - [9] M. Blanke, *et al.*, JHEP **0701**, 066 (2007).
  - [10] M. Blanke, *et al.*, JHEP **0706**, 082 (2007).
  - [11] M. Blanke, *et al.*, Phys. Lett. B **657**, 81 (2007).
  - [12] M. Blanke, *et al.*, JHEP **0705**, 013 (2007); S. R. Choudhury, *et al.*, hep-ph/0612327.
  - [13] J. Brau, Y. Okada, and N. Walker, arXiv: 0712.1950; A. Djouadi et al., arXiv:0709.1893; N. Phinney, N. Toge, and N. Walker, arXiv: 0712.2361; T. Behnke, C. Damerell, J. Jaros, and A. Myamoto, arXiv:0712.2356.
  - [14] K. Abe et al., ACFA Linear Collider Working Group, hep-ph/0109166.
  - [15] For examples, see, X. L. Wang, *et al.*, Phys. Rev. D**50**, 5781 (1994); G. R. Lu, F. R. Yin, X. L. Wang, L. D. Wan, Phys. Rev. D**68**, 015002(2003); C. S. Li, R. J. Oakes, J. M. Yang, Phys. Rev. D**49**, 293 (1994); G. Couture, C. Hamzaoui, H. Konig, Phys. Rev. D**52**, 1713 (1995); J. L. Lopez, D. V. Nanopoulos, R. Rangarajan, Phys. Rev. D**56**, 3100 (1997); G. M. de Divitiis, R. Petronzio, L. Silvestrini, Nucl. Phys. B**504**, 45 (1997); J. M. Yang, B.-L. Young, X. Zhang, Phys. Rev. D**58**, 055001 (1998); J. M. Yang, C. S. Li, Phys. Rev. D**49**, 3412 (1994); J. Guasch, J. Sola, Nucl. Phys. B**562**, 3 (1999); G. Eilam, J. L. Hewett and A. Soni, Phys. Rev. D**44**, 1473 (1991); G. Eilam, *et al.*, Phys. Lett. B**510**, 227 (2001); J. Cao, *et al.*, Phys. Rev. D**74**, 031701 (2006).
  - [16] J. Cao, Z. Xiong, J. M. Yang, Nucl. Phys. B**651**, 87 (2003); C. S. Li, X. Zhang, S. H. Zhu, Phys. Rev. D**60**, 077702 (1999).
  - [17] Z. H. Yu, *et al.*, Eur. Phys. J. C**16**, 541 (2000).
  - [18] D. Atwood, L. Reina and A. Soni, Phys. Rev. D**53**, 1199 (1996); S. Bar-Shalom, G. Eilam, A. Soni and J. Wudka, Phys. Rev. Lett. **79**, 1217 (1997); Phys. Rev. D**57**, 2957 (1998); D. Atwood, L. Reina and A. Soni, Phys. Rev. D**55**, 3156 (1997); W.-S. Hou, G.-L. Lin and C.-Y. Ma, Phys. Rev. D**56**, 7434 (1997).
  - [19] Y. Jiang, *et al.*, Phys. Rev. D**57**, 4343 (1998); W. S. Hou and G. L. Lin, Phys. Lett. B**379**, 261 (1996).
  - [20] J. Cao, G. Liu, J. M. Yang, Eur. Phys. J. C**41**, 381 (2005).
  - [21] C. Yue, Y. Dai, Q. Xu, G. Liu, Phys. Lett. B**525**, 301 (2002).
  - [22] C. Yue, G. R. Lu, J. Cao, J. Li, G. Liu, Phys. Lett. B**496**, 93 (2000).
  - [23] T. Han and J. L. Hewett, Phys. Rev. D**60**, 074015 (1999); J. A. Aguilar-Saavedra, Phys. Lett. B**502**, 115 (2001); J. A. Aguilar-Saavedra, T. Riemann, hep-ph/0102197.
  - [24] S. Bar-Shalom and J. Wudka, Phys. Rev. D**60**, 094016 (1999).

- [25] V. F. Obraztsov, S. R. Slabospitsky and O. P. Yushchenko, Phys. Lett. **B426**, 393 (1998); U. Mahanta and A. Ghosal, Phys. Rev. **D57**, 1735 (1998).
- [26] X. L. Wang, *et.al.*, Phys. Rev. **D66**, 075009 (2002); X. L. Wang, B. Z. Li, Y. L. Yang, Phys. Rev. **D68**, 115003 (2003); W. N. Xu, X. L. Wang, Z. J. Xiao, Eur. Phys. J. **C51** 891 (2007).
- [27] H. S. Hou, Phys. Rev. **D75**, 094010 (2007); X. L. Wang, Y. J. Zhang, H. L. Jin, Y. H. Xi, Nucl. Phys. **B810**, 226 (2009); X. F. Han, L. Wang, and J. M. Yang, arXiv: 0903.5491 [hep-ph].
- [28] X. L. Wang, H. L. Jin, Y. J. Zhang, Y. H. Xi, Nucl. Phys. **B807**, 210 (2009).
- [29] C. X. Yue, J. Wen, J. Y. Liu, W. Liu, hep-ph/08031335.
- [30] C. S. Huang, X. H. Wu and S. H. Zhu, Phys. Lett. **B452**, 143 (1999); C.-H Chang et al., Phys. Lett. **B313**, 389 (1993); A. Axelrod, Nucl. Phys. **B209**, 349 (1982); M. Clements et al., Phys. Rev. **D27**, 570 (1983); V. Ganapathi et al., Phys. Rev. **D27**, 579 (1983); G. Eilam, Phys. Rev. **D28**, 1202 (1983).
- [31] J. J. Cao, G. Eilam, M. Frank, K. Hikasa, G. L. Liu, I. Turan, J. M. Yang, Phys. Rev. **D75**, 075021 (2007).
- [32] G. Jikia, Nucl. Phys. **B374**, 83 (1992); O. J. P. Eboli, et al., Phys. Rev. **D47**, 1889 (1993); K. M. Cheung, *ibid.* **47**, 3750 (1993).
- [33] J. Hubisz, P. Meade, A. Noble, M. Perelstein, JHEP **0601**, 135 (2006).



## Appendix: The explicit expressions of the effective $t\bar{c}\gamma(Z)$ couplings

The effective  $t\bar{c}\gamma(Z)$  couplings  $\Gamma_{t\bar{c}\gamma}^\mu$ ,  $\Gamma_{t\bar{c}Z}^\mu$  can be directly calculated based on Fig.1, and they can be represented in form of 2-point and 3-point standard functions  $B_0, B_1, C_{ij}$ . In our calculations, the higher order  $v^2/f^2$  terms in the masses of new gauge bosons and in the Feynman rules are ignored.  $\Gamma_{t\bar{c}\gamma}^\mu$ ,  $\Gamma_{t\bar{c}Z}^\mu$  depend on the momenta of top quark and anti-charm quark( $p_t, p_{\bar{c}}$ ). Here  $p_t$  and  $p_{\bar{c}}$  are both outgoing momenta. The explicit expressions of them are

$$\Gamma_{t\bar{c}\gamma}^\mu(p_t, p_{\bar{c}}) = \Gamma_{t\bar{c}\gamma}^\mu(\eta^0) + \Gamma_{t\bar{c}\gamma}^\mu(\omega^0) + \Gamma_{t\bar{c}\gamma}^\mu(\omega^\pm) + \Gamma_{t\bar{c}\gamma}^\mu(A_H) + \Gamma_{t\bar{c}\gamma}^\mu(Z_H) + \Gamma_{t\bar{c}\gamma}^\mu(W_H^\pm) \\ + \Gamma_{t\bar{c}\gamma}^\mu(W_H^\pm\omega^\pm),$$

$$\Gamma_{t\bar{c}\gamma}^\mu(\eta^0) = \frac{i}{16\pi^2} \frac{eg'^2}{150M_{A_H}^2} (V_{Hu})_{it}^* (V_{Hu})_{ic} (A + B + C) \\ A = \frac{1}{p_t^2 - m_c^2} [m_{H_i}^2 (m_c^2 B_0^a + p_t^2 B_1^a) \gamma^\mu P_L + m_t m_c (m_{H_i}^2 B_0^a + p_t^2 B_1^a) \gamma^\mu P_R \\ + m_t (m_{H_i}^2 B_0^a + m_c^2 B_1^a) \not{p}_t \gamma^\mu P_L + m_c m_{H_i}^2 (B_0^a + B_1^a) \not{p}_t \gamma^\mu P_R] \\ B = \frac{1}{p_{\bar{c}}^2 - m_t^2} [m_{H_i}^2 (m_t^2 B_0^b + p_{\bar{c}}^2 B_1^b) \gamma^\mu P_L + m_t m_c (m_{H_i}^2 B_0^b + p_{\bar{c}}^2 B_1^b) \gamma^\mu P_R \\ - m_t m_{H_i}^2 (B_0^b + B_1^b) \gamma^\mu \not{p}_{\bar{c}} P_L - m_c (m_{H_i}^2 B_0^b + m_t^2 B_1^b) \gamma^\mu \not{p}_{\bar{c}} P_R] \\ C = m_{H_i}^2 [-\gamma^\alpha \gamma^\mu \gamma^\beta C_{\alpha\beta}^a + \gamma^\alpha \gamma^\mu (\not{p}_t + \not{p}_{\bar{c}}) C_\alpha^a + 2m_t C_\mu^a \\ - m_t \gamma^\mu (\not{p}_t + \not{p}_{\bar{c}}) C_0^a - m_{H_i}^2 \gamma^\mu C_0^a] P_L \\ + m_c [-m_t \gamma^\alpha \gamma^\mu \gamma^\beta C_{\alpha\beta}^a + m_t \gamma^\alpha \gamma^\mu (\not{p}_t + \not{p}_{\bar{c}}) C_\alpha^a + 2m_{H_i}^2 C_\mu^a \\ - m_{H_i}^2 \gamma^\mu (\not{p}_t + \not{p}_{\bar{c}}) C_0^a - m_t m_{H_i}^2 \gamma^\mu C_0^a] P_R,$$

$$\Gamma_{t\bar{c}\gamma}^\mu(\omega^0) = \frac{i}{16\pi^2} \frac{eg^2}{6M_{Z_H}^2} (V_{Hu})_{it}^* (V_{Hu})_{ic} (D + E + F) \\ D = A(B_0^a \rightarrow B_0^c, B_1^a \rightarrow B_1^c), \\ E = B(B_0^b \rightarrow B_0^d, B_1^b \rightarrow B_1^d), \\ F = C(C_{\alpha\beta}^a \rightarrow C_{\alpha\beta}^b, C_\alpha^a \rightarrow C_\alpha^b, C_0^a \rightarrow C_0^b),$$

$$\Gamma_{t\bar{c}\gamma}^\mu(\omega^\pm) = \frac{i}{16\pi^2} \frac{eg^2}{2M_{W_H}^2} (V_{Hu})_{it}^* (V_{Hu})_{ic} \left( \frac{2}{3}G + \frac{2}{3}H - \frac{1}{3}I + J \right) \\ G = A(B_0^a \rightarrow B_0^e, B_1^a \rightarrow B_1^e), \\ H = B(B_0^b \rightarrow B_0^f, B_1^b \rightarrow B_1^f), \\ I = C(C_{\alpha\beta}^a \rightarrow C_{\alpha\beta}^c, C_\alpha^a \rightarrow C_\alpha^c, C_0^a \rightarrow C_0^c), \\ J = m_{H_i}^2 [2\gamma^\alpha C_{\mu\alpha}^d - 2(m_t - \not{p}_t) C_\mu^d + (P_t + P_{\bar{c}})^\mu \gamma^\alpha C_\alpha^d \\ - (P_t + P_{\bar{c}})^\mu (m_t - \not{p}_t) C_0^d] P_L \\ + m_c [2m_t \gamma^\alpha C_{\mu\alpha}^d - 2(m_{H_i}^2 - m_t \not{p}_t) C_\mu^d + m_t (P_t + P_{\bar{c}})^\mu \gamma^\alpha C_\alpha^d \\ - (P_t + P_{\bar{c}})^\mu (m_{H_i}^2 - m_t \not{p}_t) C_0^d] P_R,$$

$$\begin{aligned}
\Gamma_{t\bar{c}\gamma}^\mu(A_H) &= \frac{i}{16\pi^2} \frac{eg'^2}{75} (V_{Hu})_{it}^* (V_{Hu})_{ic} (K + L + M) \\
K &= \frac{1}{p_t^2 - m_c^2} [p_t^2 B_1^a \gamma^\mu P_L + m_c B_1^a \not{p}_t \gamma^\mu P_R] \\
L &= \frac{1}{p_{\bar{c}}^2 - m_t^2} [p_{\bar{c}}^2 B_1^b \gamma^\mu P_L - m_t B_1^b \gamma^\mu \not{p}_{\bar{c}} P_L] \\
M &= [-\gamma^\alpha \gamma^\mu \gamma^\beta C_{\alpha\beta}^a + (\not{p}_t + \not{p}_{\bar{c}}) \gamma^\mu \gamma^\alpha C_\alpha^a - m_{Hi}^2 \gamma^\mu C_0^a] P_L,
\end{aligned}$$

$$\begin{aligned}
\Gamma_{t\bar{c}\gamma}^\mu(Z_H) &= \frac{i}{16\pi^2} \frac{eg^2}{3} (V_{Hu})_{it}^* (V_{Hu})_{ic} (N + O + P) \\
N &= K(B_1^a \rightarrow B_1^c), \\
O &= L(B_1^b \rightarrow B_1^d), \\
P &= M(C_{\alpha\beta}^a \rightarrow C_{\alpha\beta}^b, C_\alpha^a \rightarrow C_\alpha^b, C_0^a \rightarrow C_0^b),
\end{aligned}$$

$$\begin{aligned}
\Gamma_{t\bar{c}\gamma}^\mu(W_H^\pm) &= \frac{i}{16\pi^2} \frac{eg^2}{2} (V_{Hu})_{it}^* (V_{Hu})_{ic} \left( \frac{4}{3} Q + \frac{4}{3} R - \frac{2}{3} S - T \right) \\
Q &= K(B_1^a \rightarrow B_1^e), \\
R &= L(B_1^b \rightarrow B_1^f), \\
S &= M(C_{\alpha\beta}^a \rightarrow C_{\alpha\beta}^c, C_\alpha^a \rightarrow C_\alpha^c, C_0^a \rightarrow C_0^c) \\
T &= \{4\gamma^\alpha C_{\mu\alpha}^d + [\gamma^\mu \not{p}_t \gamma^\alpha - \gamma^\mu \gamma^\alpha \not{p}_t + 2\not{p}_t \gamma^\alpha \gamma^\mu + \gamma^\alpha \not{p}_t \gamma^\mu - \gamma^\mu \gamma^\alpha \not{p}_{\bar{c}} \\
&\quad + 2\not{p}_{\bar{c}} \gamma^\alpha \gamma^\mu + 2(p_t + p_{\bar{c}})^\mu \gamma^\alpha] C_\alpha^d + 4\not{p}_t C_\mu^d + 2(B_0^g + m_{WH}^2 C_0^d) \gamma^\mu \\
&\quad + [2\not{p}_{\bar{c}} \not{p}_t \gamma^\mu - \gamma^\mu \not{p}_t \not{p}_{\bar{c}} + 2\not{p}_t (p_t + p_{\bar{c}})^\mu + p_t^2 \gamma^\mu] C_0^d\} P_L,
\end{aligned}$$

$$\begin{aligned}
\Gamma_{t\bar{c}\gamma}^\mu(W_H^\pm \omega^\pm) &= \frac{i}{16\pi^2} \frac{eg^2}{2} (V_{Hu})_{it}^* (V_{Hu})_{ic} \\
&\quad \times \{ [m_t \not{p}_t C_0^d + m_t \gamma^\alpha C_\alpha^d - 2m_{Hi}^2 C_0^d] \gamma^\mu P_L + m_c [\gamma^\mu \not{p}_t C_0^d + \gamma^\mu \gamma^\alpha C_\alpha^d] P_R \},
\end{aligned}$$

$$\begin{aligned}
\Gamma_{t\bar{c}Z}^\mu(p_t, p_{\bar{c}}) &= \Gamma_{t\bar{c}Z}^\mu(\eta^0) + \Gamma_{t\bar{c}Z}^\mu(\omega^0) + \Gamma_{t\bar{c}Z}^\mu(\omega^\pm) + \Gamma_{t\bar{c}Z}^\mu(A_H) + \Gamma_{t\bar{c}Z}^\mu(Z_H) + \Gamma_{t\bar{c}Z}^\mu(W_H^\pm) \\
&\quad + \Gamma_{t\bar{c}Z}^\mu(W_H^\pm \omega^\pm),
\end{aligned}$$

$$\begin{aligned}
\Gamma_{t\bar{c}Z}^\mu(\eta^0) &= \frac{i}{16\pi^2} \frac{g}{\cos\theta_W} \frac{g'^2}{100M_{A_H}^2} (V_{Hu})_{it}^* (V_{Hu})_{ic} (A' + B' + C') \\
A' &= \frac{1}{p_t^2 - m_c^2} \left[ \left( \frac{1}{2} - \frac{2}{3} \sin^2\theta_W \right) m_{H_i}^2 (m_c^2 B_0^a + p_t^2 B_1^a) \gamma^\mu P_L \right. \\
&\quad \left. - \frac{2}{3} \sin^2\theta_W m_t m_c (m_{H_i}^2 B_0^a + p_t^2 B_1^a) \gamma^\mu P_R \right. \\
&\quad \left. + \left( \frac{1}{2} - \frac{2}{3} \sin^2\theta_W \right) m_t (m_{H_i}^2 B_0^a + m_c^2 B_1^a) \not{p}_t \gamma^\mu P_L \right. \\
&\quad \left. - \frac{2}{3} \sin^2\theta_W m_c m_{H_i}^2 (B_0^a + B_1^a) \not{p}_t \gamma^\mu P_R \right] \\
B' &= \frac{1}{p_{\bar{c}}^2 - m_t^2} \left[ \left( \frac{1}{2} - \frac{2}{3} \sin^2\theta_W \right) m_{H_i}^2 (m_t^2 B_0^b + p_{\bar{c}}^2 B_1^b) \gamma^\mu P_L \right. \\
&\quad \left. - \frac{2}{3} \sin^2\theta_W m_t m_c (m_{H_i}^2 B_0^b + p_{\bar{c}}^2 B_1^b) \gamma^\mu P_R \right. \\
&\quad \left. + \frac{2}{3} \sin^2\theta_W m_t m_{H_i}^2 (B_0^b + B_1^b) \gamma^\mu \not{p}_{\bar{c}} P_L \right. \\
&\quad \left. - \left( \frac{1}{2} - \frac{2}{3} \sin^2\theta_W \right) m_c (m_{H_i}^2 B_0^b + m_t^2 B_1^b) \gamma^\mu \not{p}_{\bar{c}} P_R \right] \\
C' &= \left( \frac{1}{2} - \frac{2}{3} \sin^2\theta_W \right) C,
\end{aligned}$$

$$\begin{aligned}
\Gamma_{t\bar{c}Z}^\mu(\omega^0) &= \frac{i}{16\pi^2} \frac{g}{\cos\theta_W} \frac{g^2}{4M_{Z_H}^2} (V_{Hu})_{it}^* (V_{Hu})_{ic} (D' + E' + F') \\
D' &= A'(B_0^a \rightarrow B_0^c, B_1^a \rightarrow B_1^c), \\
E' &= B'(B_0^b \rightarrow B_0^d, B_1^b \rightarrow B_1^d), \\
F' &= C'(C_{\alpha\beta}^a \rightarrow C_{\alpha\beta}^b, C_\alpha^a \rightarrow C_\alpha^b, C_0^a \rightarrow C_0^b),
\end{aligned}$$

$$\begin{aligned}
\Gamma_{t\bar{c}Z}^\mu(\omega^\pm) &= \frac{i}{16\pi^2} \frac{g}{\cos\theta_W} \frac{g^2}{2M_{W_H}^2} (V_{Hu})_{it}^* (V_{Hu})_{ic} (G' + H' + I' + J') \\
G' &= A'(B_0^a \rightarrow B_0^e, B_1^a \rightarrow B_1^e), \\
H' &= B'(B_0^b \rightarrow B_0^f, B_1^b \rightarrow B_1^f), \\
I' &= \left( -\frac{1}{2} + \frac{1}{3} \sin^2\theta_W \right) I, \\
J' &= \cos^2\theta_W J,
\end{aligned}$$

$$\begin{aligned}
\Gamma_{t\bar{c}Z}^\mu(A_H) &= \frac{i}{16\pi^2} \frac{g}{\cos\theta_W} \frac{g'^2}{50} (V_{Hu})_{it}^* (V_{Hu})_{ic} (K' + L' + M') \\
K' &= \frac{1}{p_t^2 - m_c^2} \left[ \left( \frac{1}{2} - \frac{2}{3} \sin^2\theta_W \right) p_t^2 B_1^a \gamma^\mu P_L - \frac{2}{3} \sin^2\theta_W m_c B_1^a \not{p}_t \gamma^\mu P_R \right] \\
L' &= \frac{1}{p_{\bar{c}}^2 - m_t^2} \left[ \left( \frac{1}{2} - \frac{2}{3} \sin^2\theta_W \right) p_{\bar{c}}^2 B_1^b \gamma^\mu P_L + \frac{2}{3} \sin^2\theta_W m_t B_1^b \not{p}_{\bar{c}} \gamma^\mu P_L \right] \\
M' &= \left( \frac{1}{2} - \frac{2}{3} \sin^2\theta_W \right) \left[ -\gamma^\alpha \gamma^\mu \gamma^\beta C_{\alpha\beta}^a + (\not{p}_t + \not{p}_{\bar{c}}) \gamma^\mu \gamma^\alpha C_\alpha^a - m_{H_i}^2 C_0^a \gamma^\mu \right] P_L,
\end{aligned}$$

$$\Gamma_{t\bar{c}Z}^\mu(Z_H) = \frac{i}{16\pi^2} \frac{g}{\cos\theta_W} \frac{g^2}{2} (V_{Hu})_{it}^* (V_{Hu})_{ic} (N' + O' + P')$$

$$N' = K'(B_1^a \rightarrow B_1^c),$$

$$O' = L'(B_1^b \rightarrow B_1^d),$$

$$P' = M'(C_{\alpha\beta}^a \rightarrow C_{\alpha\beta}^b, C_\alpha^a \rightarrow C_\alpha^b, C_0^a \rightarrow C_0^b),$$

$$\Gamma_{t\bar{c}Z}^\mu(W_H^\pm) = \frac{i}{16\pi^2} \frac{g}{\cos\theta_W} g^2 (V_{Hu})_{it}^* (V_{Hu})_{ic} (Q' + R' + S' + T')$$

$$Q' = K'(B_1^a \rightarrow B_1^e),$$

$$R' = L'(B_1^b \rightarrow B_1^f),$$

$$S' = \left(-\frac{1}{2} + \frac{1}{3} \sin^2\theta_W\right) S,$$

$$T' = -\frac{1}{2} \cos^2\theta_W T,$$

$$\Gamma_{t\bar{c}Z}^\mu(W_H^\pm \omega^\pm) = \frac{i}{16\pi^2} g \cos\theta_W \frac{g^2}{2} (V_{Hu})_{it}^* (V_{Hu})_{ic}$$

$$\times \{[m_t \not{p}_t C_0^d + m_t \gamma^\alpha C_\alpha^d - 2m_{H_i}^2 C_0^d] \gamma^\mu P_L + m_c [\gamma^\mu \not{p}_t C_0^d + \gamma^\mu \gamma^\alpha C_\alpha^d] P_R\}.$$

For the two-point and three-point standard loop functions  $B_0, B_1, C_0, C_{ij}$  in the above expressions are defined as

$$B^a = B^a(-p_t, m_{H_i}, M_{A_H}), B^b = B^b(-p_{\bar{c}}, M_{H_i}, M_{A_H}),$$

$$B^c = B^c(-p_t, m_{H_i}, M_{Z_H}), B^d = B^d(-p_{\bar{c}}, M_{H_i}, M_{Z_H}),$$

$$B^e = B^e(-p_t, m_{H_i}, M_{W_H}), B^f = B^f(-p_{\bar{c}}, M_{H_i}, M_{W_H}),$$

$$B^g = B^g(p_{\bar{c}}, M_{H_i}, M_{W_H}),$$

$$C_{ij}^a = C_{ij}^a(-p_t, -p_{\bar{c}}, m_{H_i}, M_{A_H}, m_{H_i}),$$

$$C_{ij}^b = C_{ij}^b(-p_t, -p_{\bar{c}}, m_{H_i}, M_{Z_H}, m_{H_i}),$$

$$C_{ij}^c = C_{ij}^c(-p_t, -p_{\bar{c}}, m_{H_i}, M_{W_H}, m_{H_i}),$$

$$C_{ij}^d = C_{ij}^d(p_t, p_{\bar{c}}, M_{W_H}, m_{H_i}, M_{W_H}).$$

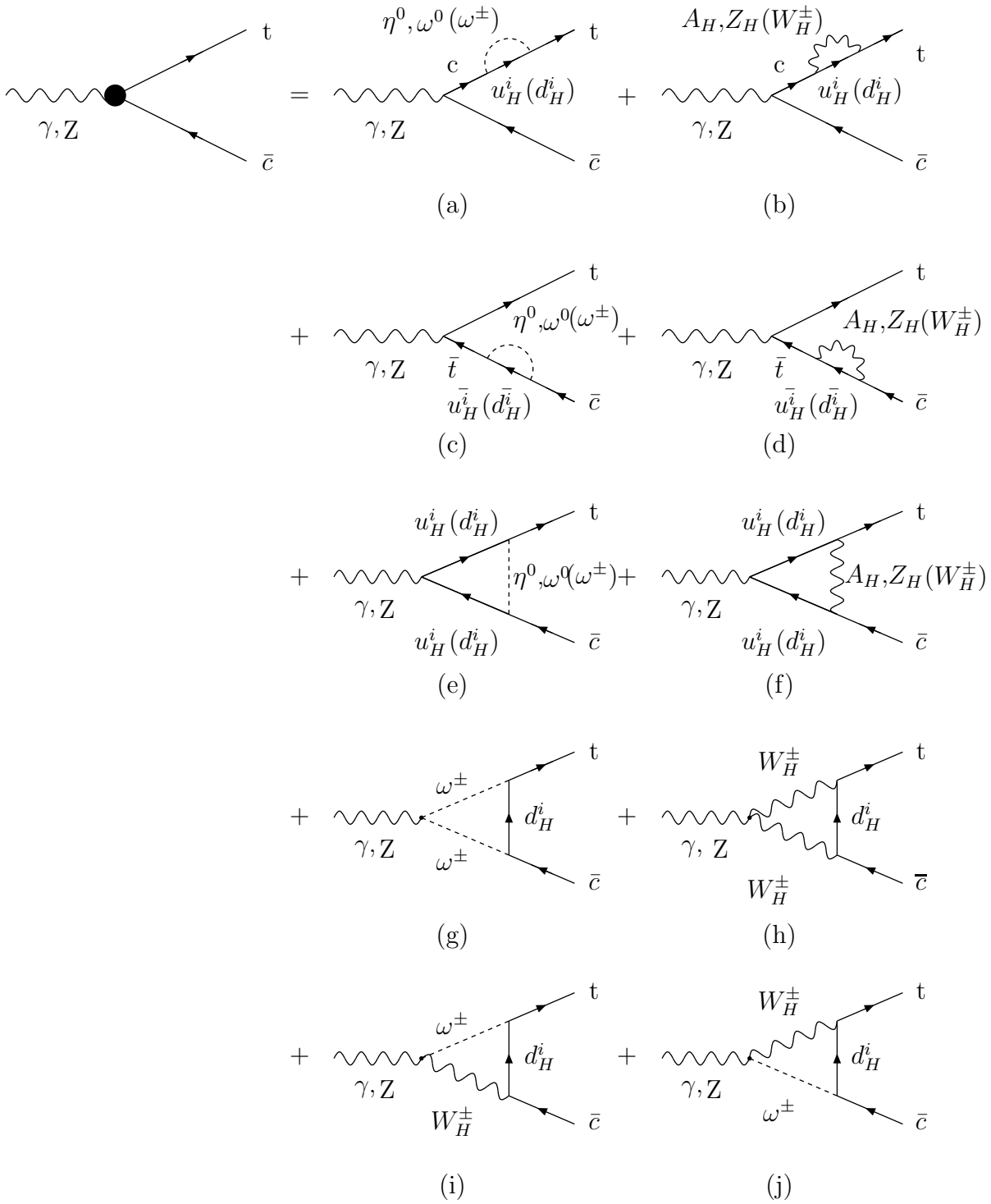


FIG. 1: One-loop contributions of the LHT model to the couplings  $t\bar{c}\gamma(Z)$ .

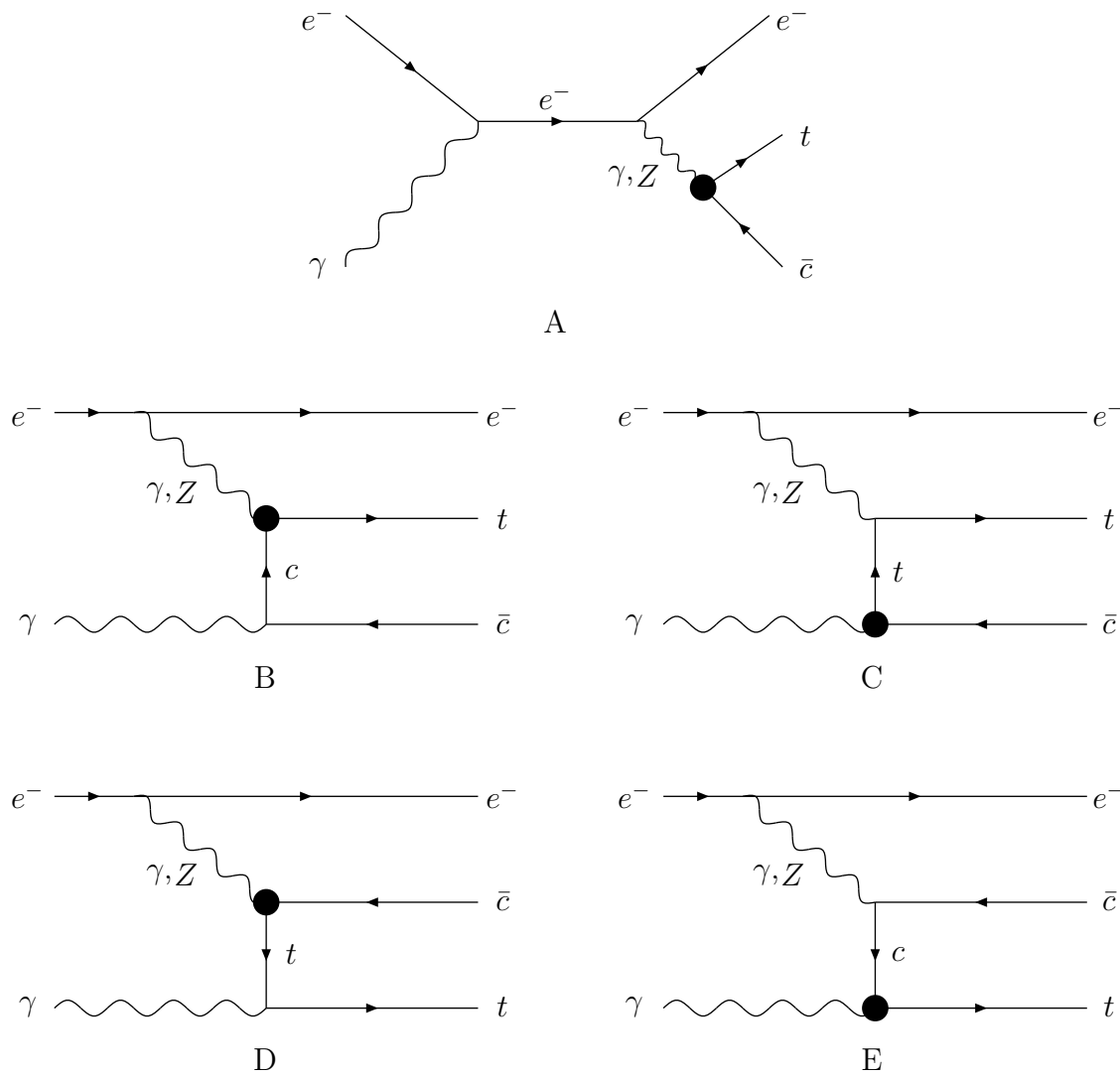


FIG. 2: The Feynman diagrams for  $e^- \gamma \rightarrow e^- t \bar{c}$  in the LHT model.

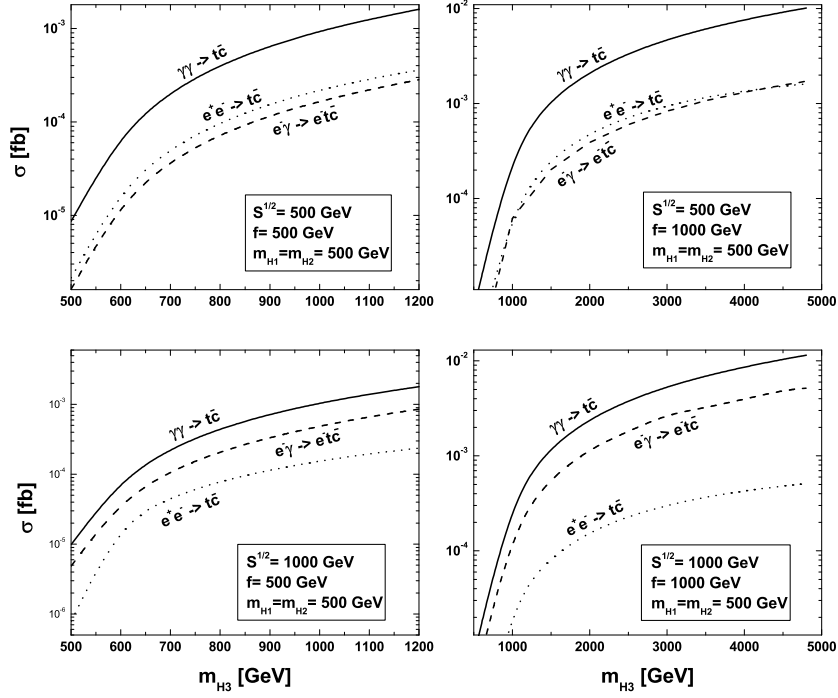


FIG. 3: The cross sections of top-charm associated production processes versus  $m_{H_3}$  in the LHT model for Case I.

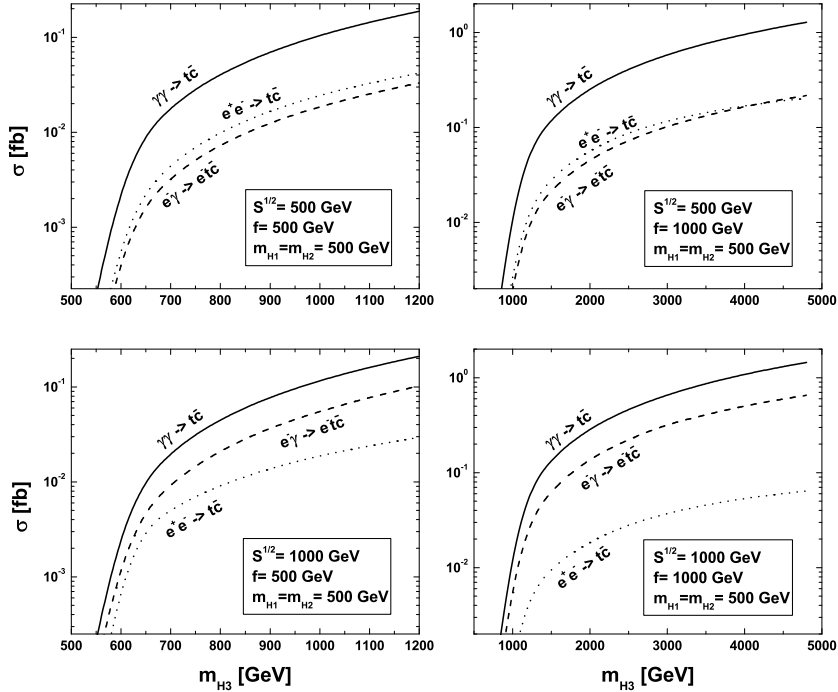


FIG. 4: The cross sections of top-charm associated production processes versus  $m_{H_3}$  in the LHT model for Case II.

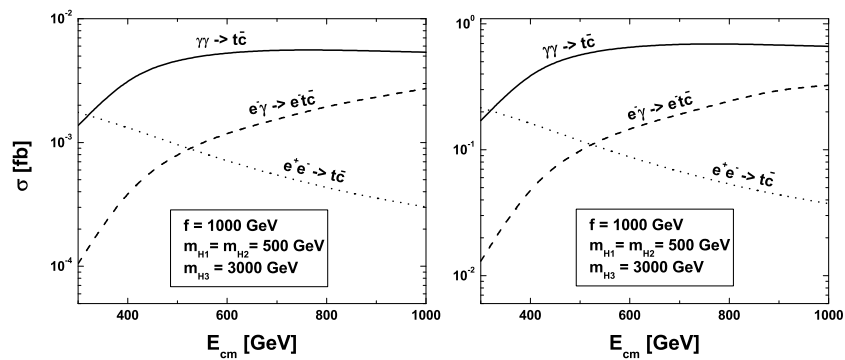


FIG. 5: Cross sections versus collider energy  $E_{cm} = \sqrt{s_{ee}}$  in the LHT model. The left diagram is for Case I and the right diagram is for Case II.